



Nanoparticles of Cadmium Sulfide in Mesoporous SBA-15 Host: Preparation and Characterization

HUI YU, SHUN HU, XIAO-DONG LI and QING-ZHOU ZHAI*

Research Center for Nanotechnology, Changchun University of Science and Technology, 7186 Weixing Road, Changchun 130022, P.R. China

*Corresponding author: Fax: +86 431 85383815; Tel: +86 431 85583118; E-mail: zhaiqingzhou@163.com; zhaiqingzhou@hotmail.com

(Received: 19 January 2011;

Accepted: 25 July 2011)

AJC-10205

In this research, cadmium sulfide nanoparticles were introduced into the mesoporous SBA-15 by ion exchange and hydrothermal method. Characterization by chemical analysis, infrared spectra, powder X-ray diffraction, nitrogen adsorption-desorption, scanning electron microscopy and photoluminescence study indicates that the guest cadmium sulfide has been located in the host channels of host-guest (SBA-15)-CdS nanocomposite materials. The SEM results indicated that the average size of (SBA-15)-CdS was 323 nm. The photoluminescence study revealed that at 541 nm the nanocomposite compounds (SBA-15)-CdS show luminescence and have an applied foreground as a promising luminescent material.

Key Words: Cadmium sulfide nanoparticle, SBA-15 molecular sieve, Host-guest nanocomposite material.

INTRODUCTION

The new type functional materials having physical and chemical functions such as light, electricity, magnetism, heat, *etc.*, have caused people's wide concerns. These materials deal with biological medical materials, nanomedical carrier materials, optical electrical functional materials, magnetic functional materials, hydrogen-storage materials, functional films materials, fibre materials, semiconductor materials, *etc.*¹. In recent years, scientists made a great deal of studies on ultramicro quantum effect of new type semiconductor materials and of nanostructure systems, finding many new phenomena and achieving remarkable substantial achievements. At present, functionalized guest materials are incorporated into long-range ordered pore materials to obtain the materials having new type functions, which will become one of frontier fields of nanoscience². The properties of this kind of new type nanocomposite materials are mainly determined by the properties of guest material. Also, the ordered nanopores also take great effect on the physical chemical properties of the nanomaterials. By different chemical environment, constructing different geometric configurational pore channel structure can very well control the chemical, physical properties of host-guest materials. SBA-15 is a very interesting molecular sieve and it has a series of advantages. It has larger channels (5-30 nm) and is easily synthesized, *etc.*^{3,4}. Its channels are specially suitable to be used as host material for manufacturing nanostructures. It caused people's great interests that guests materials are

incorporated in molecular sieve type materials to manufacture host-guest composite materials. It has been reported that La_2O_3 ², nimodipine drug⁵ were incorporated into SBA-15, metals^{6,7}, dye⁸, C_{60} fullrene⁹, CeO_2 ¹⁰ were incorporated into MCM-41 and CoS ¹¹ was incorporated into ZSM-5. In recent years, the study that proteins were encapsulated in mesoporous materials¹²⁻¹⁵ caused scientists' interests. CdS is a II-VI family semiconductor compound, having a potential applied foreground as optical catalytic materials¹⁶. It has been incorporated into MCM-41¹⁶. It is expected that the nanostructured CdS produced inside molecular sieve channels should have higher optical catalytic activity and has higher applied value. The present study uses SBA-15 molecular sieve as host and exchanges Cd^{2+} into SBA-15 by ion-exchange method. Thioacetamide is used as sulfur source to make Cd-(SBA-15) sulfidation by hydrothermal method and (SBA-15)-CdS is prepared. Chemical analysis, IR, powder XRD, 77 K low temperature nitrogen adsorption-desorption, SEM and photoluminescence study were employed to characterize the nanocomposite materials prepared. The present method uses thioacetamide as sulfur source to avoid the toxicity of direct sulfidation of H_2S and has the advantages of operation simplicity and easiness. It has better practical value.

EXPERIMENTAL

Tricopolymerpoly(ethylene glycol)-block-poly(propyl glycol)-block-poly(ethylene glycol) ($\text{EG}_{20}\text{PG}_{40}\text{EG}_{20}$, average molecular weight 5800, Aldrich); 2 mol/L of hydrochloric acid

solution (AR, Changchun Chemical Leechdom Corporation, Ltd., China); tetraethyl orthosilicate (TEOS, 98 %, Fluka); trimethylchlorosilane (AR, Shanghai Chemical Corporation of Chinese Medicine Group, China); CdCl_2 (AR, Shanghai Chemical Corporation of Chinese Medicine Group, China); absolute ethanol (AR, Changchun Chemical Reagent Plant, China); thioacetamide (AR, Shanghai Lingfeng Chemical Reagent Corporation, Ltd., China); the deionized water used in the experiments whose electric conductivity was 0.08 $\mu\text{S}/\text{cm}$.

Preparation of SBA-15 molecular sieve: Mesoporous SBA-15 molecular sieve was prepared according to the procedure^{3,4}. In the acidic condition, the triblock copolymer, $\text{EG}_{20}\text{PG}_{40}\text{EG}_{20}$ was used as template and TEOS was used as silica source. In a typical synthesis, 2 g of the template was dissolved in 60 g of 2 mol/L hydrochloric acid and 15 g of deionized water, then 4.25 g of TEOS was added, stirred for 24 h at 40 °C. The mixture was kept in a Teflon-liner autoclave treated at 100 °C for 48 h. The product was filtered and washed with deionized water and dried at room temperature. The material was calcined at 550 °C for 24 h to completely eliminate the template.

The outside surface of the SBA-15 molecular sieve was modified by trimethylchlorosilane before calcination. After the reaction, the silanol groups of the SBA-15 surface were replaced by CH_3 - group of trimethylchlorosilane. Then, the sample was calcined at 550 °C for 24 h. The purpose was to eliminate the template and the silane was oxidized from the outside surface of the SBA-15. In this work, for the modification of the SBA-15 with silane prior calcination, it is expected that all of the silane can be oxidized from the outside surface of the SBA-15, but the silanol groups of the inner surface of the pore channels can be kept. The purpose was that CdS was grafted on the inner surface of the pore channels of the SBA-15 but not grafted on the outside surface of the SBA-15.

The procedure for the preparation of modified SBA-15 material is as follows: 0.5 g of the uncalcined mesoporous SBA-15 powder was immersed in 15 mL of 1 % (v/v) trimethylchlorosilane absolute ethanol solution and stirred for 24 h at room temperature. The solid product was filtered off, washed with absolute ethanol solution and dried at room temperature. The obtained material was calcined at 550 °C for 24 h.

Preparation of (SBA-15)-CdS nanocomposite material:

In a 50 mL beaker, 0.3 g of SBA-15 was added into 0.1 mol/L CdCl_2 ethanol-water solution (volume ratio, 1:1) with stirring for 24 h at ambient temperature. Then, the above substance was filtered and washed. After that, the solid was dried at 60 °C for 6 h. The above sample was taken, placed in 30 mL 0.1 mol/L thioacetamide solution. The mixture was placed and sealed in the autoclave and heated at 80 °C for 48 h, then the resulting product was washed by deionized water. The obtained solid sample was dried at 60 °C for 6 h. The host-guest composite material prepared was designed as (SBA-15)-CdS.

Characterization: Determination of cadmium in the (SBA-15)-CdS nanocomposite material was made on a Japanese Hitachi Z-8000 polarization atomic absorption spectrometer. The content of oxygen element was determined by German VERIOEL elemental analyzer. The silicon content was determined by using molybdosilicate blue photometry¹⁷. Fourier

transform infrared (FT-IR) spectra were obtained using German BRUKER Vertex-70 spectrometer with 4 cm^{-1} resolution. Powder samples were dispersed in KBr pellets for IR analysis. The phase composition of the solid products was determined by X-ray diffraction on a German D5005 diffractometer (Siemens Company) equipped with graphite-monochromator $\text{CuK}\alpha$ radiation. Nitrogen adsorption-desorption isotherms were determined at 77 K using an adsorption porosimeter (Micromeritics ASAP2010M, American Mike Company). The surface area measurements were performed according to the Brunner-Emmett-Teller (BET) method. Pore size distribution was obtained by applying the Barrett-Joyner-Halenda (BJH) method. Scanning electron micro-graphies were performed using a Japanese Hitachi JEOL JSM-5600L. Room temperature (25 °C) photoluminescence spectra were measured on a PEX-FL-2T-2 (American SPEX Company) spectrofluorophotometer.

RESULTS AND DISCUSSION

Chemical analysis: A content of cadmium in the (SBA-15)-CdS determined by atomic absorption spectrometry was 7.30 %. The sulfur content was determined by gravimetric method was 2.08 %. A content of silicon determined by molybdosilicate blue photometry was 42.29 %. A content of oxygen determined by elemental analysis method was 48.33 %. The content of cadmium sulfide was 9.38 %. The molar ratio of Cd:S was 1:1. This shows that CdS incorporated into SBA-15 molecular sieve host.

Infrared spectra: The FT-IR spectra of SBA-15, uncalcined trimethylchlorosilane-modified SBA-15 and calcined trimethylchlorosilane-modified SBA-15 are given in Fig. 1. As shown in curve C, before calcination of trimethylchlorosilane-modified SBA-15 a band appeared at 2965 cm^{-1} due to methyl C-H characteristic IR peak⁴. This shows that the surface silanol was replaced by $-\text{CH}_3$. However, after calcination of 550 °C, $-\text{CH}_3$ was oxidized and broke away from the frame-

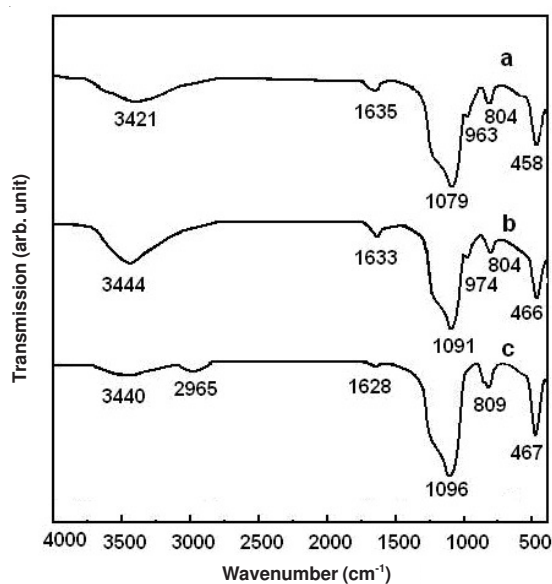


Fig. 1. Infrared spectra of the samples: (a) SBA-15; (b) post modification sample by chlorotrimethylsilane (calcined); (c) post modification sample by chlorotrimethylsilane (uncalcined)

work of the molecular sieve. The peak at 963 cm^{-1} is assigned to the stretching of silanol groups O-H of the SBA-15, the peak disappeared for the sample before calcination. This shows that the silanol groups have been replaced by the methyl group. Similar peaks for the calcined sample appeared (curve B) compared with those of SBA-15 molecular sieve (curve A), which indicates that the modified SBA-15 has the same framework with the SBA-15 molecular sieve and the silanol groups of the inner surface of the pore channels have been well kept. The infrared spectra of SBA-15, CdS and (SBA-15)-CdS are given in Fig. 2. Compared with curve C with A and B, it is found that the infrared spectrum of (SBA-15)-CdS sample did not show the characteristic peak of CdS, showing that CdS uniformly dispersed in the channels of molecular sieve and no aggregated nanoscale crystal formed. The CdS existed in the form of quantum dots or quantum strings.

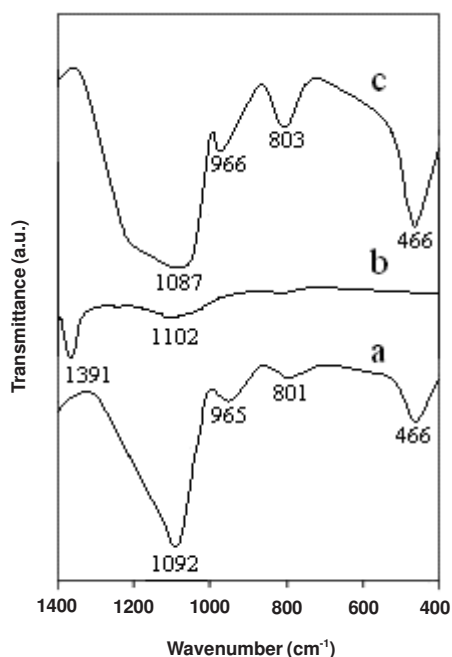


Fig. 2. Infrared spectra of the samples: (a) SBA-15; (b) CdS; (c) (SBA-15)-CdS

Powder X-ray diffraction: A feasible method to confirm whether the cadmium sulfide is encapsulated in the pores of the SBA-15 or not, is the analysis of the host before and after encapsulation by XRD and nitrogen physisorption to indicate the stability of the host and the extent of pore filling. Powder XRD patterns of a series of samples in the range of $0-10^\circ$ are shown in Fig. 3. The three samples exhibit the typical diffraction peaks of SBA-15 molecular sieve and have high intensities. However, the intensity gradually decreased in the order of SBA-15, (SBA-15)-Cd, (SBA-15)-CdS. Generally speaking, the introduction of scattering material into the pores leads to an increased phase cancellation between scattering from the wall and the pore regions and therefore to reduce scattering intensities for the Bragg reflections. Theoretical models have shown that this phase relationship is very sensitive. The degree of cancellation is mainly determined by the scattering contrast between the framework walls and the pores^{18,19}. Curve A shows three relatively weak diffraction peaks (110), (200), (210),

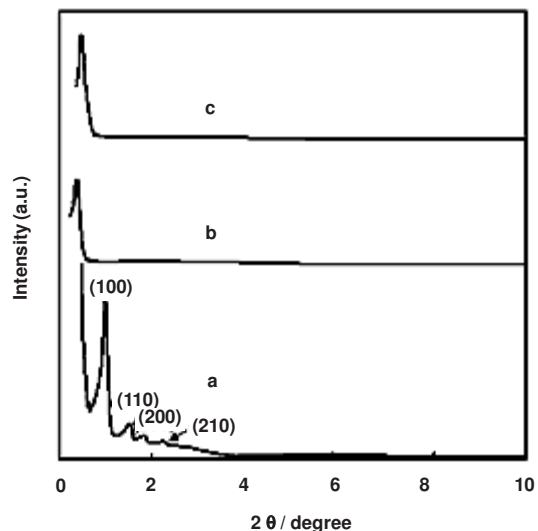


Fig. 3. Small angle XRD patterns of the samples: (a) SBA-15; (b) (SBA-15)-Cd; (c) (SBA-15)-CdS

indicating that high quality of SBA-15 material has been successfully prepared. Fig. 3 shows that the long range ordering of crystal lattice of (SBA-15)-CdS nanocomposite material was still very high after the incorporation of CdS. However, disappearance of (110), (200) and (210) diffraction peaks suggests that the incorporation of CdS into SBA-15 resulted in decrease in the ordered degree of the molecular sieve but did not destroy the framework of SBA-15 molecular sieve. Fig. 4 is the wide-angle XRD pattern for the (SBA-15)-CdS sample over the range of $10-80^\circ$, showing broad characteristic peaks belonging to the CdS nanoparticles²⁰⁻²². This indicates that cadmium sulfide has been incorporated into the SBA-15. On the basis of the width of the diffraction peaks, the average size of the cadmium sulfide nanoparticles is estimated to be 3 nm.

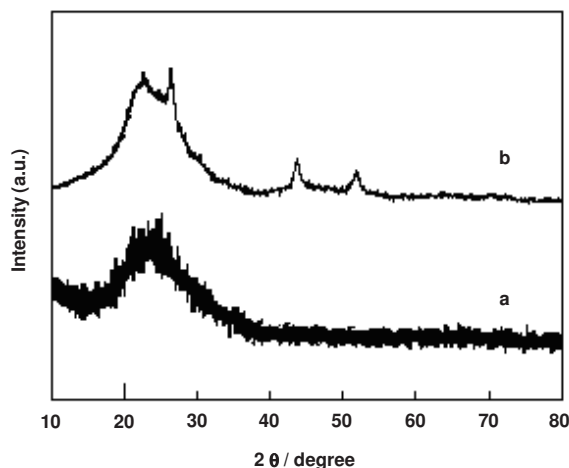


Fig. 4. Wide angle XRD patterns of the samples: (a) SBA-15; (b) nanoscale CdS encapsulated in SBA-15

Nitrogen physisorption and scanning electron microscopic study: Fig. 5 presents the low temperature N_2 adsorption-desorption isotherms of SBA-15 (curve A) and (SBA-15)-CdS (curve B). From the figure it can be known that the isotherms belong to Langmuir IV type isotherm and are typical characteristic adsorption curve of mesoporous molecular sieve. At

the same time in the section of middle pressure an H1 type hysteresis loop appeared. In low pressure section ($P/P_0 < 0.59$), the adsorbed amount of nitrogen gas assumed a linear relationship increase as P/P_0 increased but the slope of adsorption ratio was gentle, because nitrogen molecules formed single layer adsorption inside the pore channels of molecular sieve and the adsorbed amount of nitrogen molecules was not large. In a middle pressure section ($0.59 < P/P_0 < 0.79$), N_2 molecules formed multilayer adsorption in inner pore walls of the molecular sieve and thus the adsorbed amount of N_2 suddenly increased as relative pressure increased. For the adsorption-desorption curves break took place and obvious inflection point appeared. At the same time, as the adsorbed amount of nitrogen gas molecules was more than the desorbed amount of nitrogen gas molecules, so a hysteresis loop formed. This shows that capillary condensation phenomenon took place for nitrogen molecules inside the SBA-15 channels in (SBA-15)-CdS. Afterwards, when $P/P_0 > 0.79$, adsorption and desorption curves coincided and increase was slow. The adsorption of nitrogen molecules also gradually reached saturation and nitrogen molecules began to be adsorbed on outside surface of the molecular sieve. Therefore, it can be seen from the above phenomena that (SBA-15)-CdS nanocomposite material still kept the framework structure of SBA-15 molecular sieve. The capillary condensation phenomenon over the range of $0.59 < P/P_0 < 0.79$ shows that the pore channels of (SBA-15)-CdS still was in the range of mesoporous channels and pore size distribution was narrower. CdS homogeneously distributed inside the channels of SBA-15. Fig. 6 is the pore size distribution patterns of modified-SBA-15 and (SBA-15)-CdS. The results suggest that the pore channels present one-dimensional ordered mesoporous channels and pore size distribution is narrow. Table-1 and Fig. 5 show that the mean pore diameter and the pore volume decreased, respectively from 6.76 nm and 1.13 cm^3/g for modified SBA-15 to 6.01 nm and 0.93 cm^3/g for (SBA-15)-CdS. A decrease of specific surface area was also observed from 659 m^2/g for SBA-15 to 477 m^2/g for the hybrid host-guest composite material. These results suggest that cadmium sulfide can be confined within the SBA-15 pore channels. As (SBA-15)-CdS nanocomposite material has uniform pore size distribution, the molecular sieve after incorporation of CdS still has the characteristics of mesoporous material. The structure parameters of samples, pore volume, pore size, specific surface area, etc., are listed in Table-1.

Fig. 7 is the scanning electron microscopic images of the sample (SBA-15)-CdS. There was not aggregated CdS molecules on its surface. Its shape was fibriform and its average size was 323 nm.

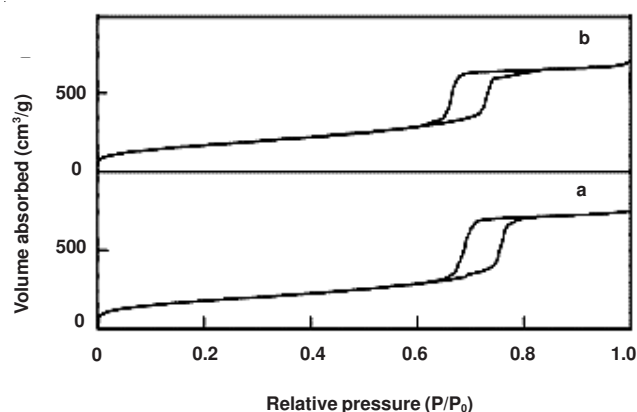


Fig. 5. Low temperature nitrogen adsorption-desorption isotherms of the samples: (a) SBA-15; (b) (SBA-15)-CdS

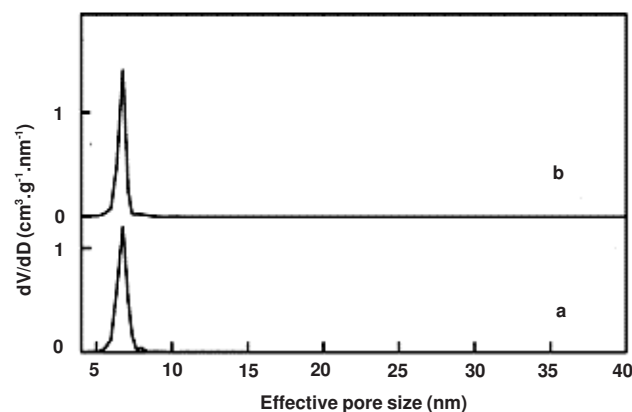


Fig. 6. Pore size distribution patterns of the samples: SBA-15; (b) (SBA-15)-CdS

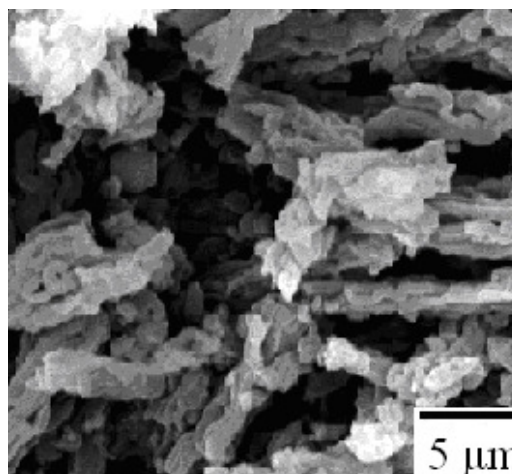


Fig. 7. SEM images of (SBA-15)-CdS sample

TABLE-1
PORE STRUCTURE PARAMETERS OF THE SAMPLES

Sample	Crystal face spacing / d_{100} (nm)	Unit cell parameter/ a_0^a (nm)	BET surface area (m^2/g)	Pore volume ^b (cm^3/g)	Pore size ^c (nm)	Wall thickness ^d (nm)	Content of CdS (wt. %)
Modified SBA-15	10.91	12.60	659	1.13	6.76	5.84	0
(SBA-15)-CdS	17.17	19.83	477	0.93	6.01	13.82	9.38

a: Unit cell parameter], $a_0 = \frac{2}{\sqrt{3}}d_{100}$. B: BJH adsorption cumulative volume of pores. c: Pore size calculated from the adsorption branch. d: Wall thickness calculated by (a_0 - pore size).

Photoluminescence study: The excitation and emission spectra of (SBA-15)-CdS are shown in Fig. 8. It can be seen that the emission band of sample was broad over the range of 200-800 nm, showing the existence of defects in the sample. The non-radiative process in the sample is strong and Stokes shift happened, which widens the spectrum bands. As semiconductor CdS was encapsulated in the nanopore channels of SBA-15, thus due to the small size effect, the luminescent effect of nanoparticles was influenced. Smaller size of CdS particles, larger its energy gap. After semiconductor CdS was excited, the sulfur atoms near surface thermally moved to the surface, vacant position put apart in the primary sulfur place. Then, inner neighbour electrons easily moved into the vacant position, resulting in Schottky defects. At the same time, the going of the electrons resulted in appearance of cavities. Therefore, the cavities were excited by the resonance of SBA-15 at 541 nm and very strong emission peak appeared.

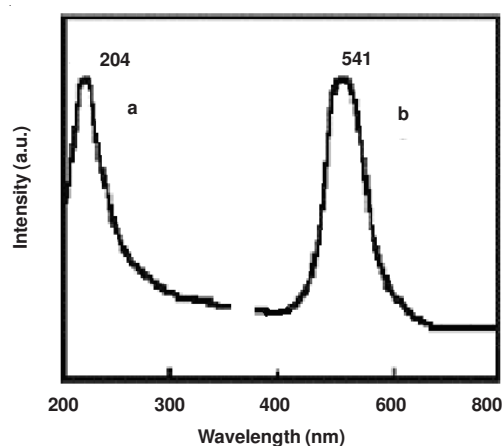


Fig. 8. Luminescence of the(SBA-15)-CdS sample: (a) excitation spectrum; (b) emission spectrum

Conclusion

The (SBA-15)-CdS samples were prepared by ion exchange and hydrothermal method. A series of characterizations including

chemical analysis, infrared spectroscopy, powder XRD, N_2 adsorption technique, SEM and photoluminescence study showed that cadmium sulfide nanoparticles have been situated in the mesoporous SBA-15 pores. The average size of (SBA-15)-CdS was 323 nm. At 541 nm, the nanocomposite compounds (SBA-15)-CdS show luminescence, having an applied foreground as a luminescent material.

REFERENCES

1. Q. Z. Zhai, Nanotechnology, Beijing: Weapon Industry Press, p. 23 (2006).
2. H. Yu and Q.Z. Zhai, *J. Solid State Chem.*, **181**, 2424 (2008).
3. D.Y. Zhao, J.L. Feng, Q.S. Huo, B.F. Chmelka and G.D. Stucky, *J. Am. Chem. Soc.*, **120**, 6024 (1998).
4. D.Y. Zhao, J.L. Feng, Q.S. Huo, N. Melosh, G.H. Fredrickson, B.F. Chmelka and G.D. Stucky, *Science*, **279**, 548 (1998).
5. H. Yu and Q.Z. Zhai, *Micropor. Mesopor. Mater.*, **123**, 298 (2009).
6. Y.P. Hsieh, J.W. Chen, C.T. Liang, Y.F. Chen, A.Q. Wang and C.Y. Mou, *J. Lumin.*, **128**, 553 (2008).
7. A. Pourahmad and S. Sohrabnezhad, *J. Alloys. Compd.*, **484**, 314 (2009).
8. Q.D. Qin, J. Ma and K. Liu, *J. Hazard. Mater.*, **162**, 133 (2009).
9. S. Minakata, R. Tsuruoka and M. Komatsu, *J. Am. Chem. Soc.*, **130**, 1536 (2008).
10. X.L. Song, P. Qu, N. Jiang, H.M. Yang and G.Z. Qiu, *Colloids. Surf. A*, **313-314**, 193 (2008).
11. S. Sohrabnezhad, A. Pourahmad and M.A. Zanjanchi, *J. Iran. Chem. Soc.*, **6**, 612 (2009).
12. D. Jung, C. Streb and M. Hartmann, *Micropor. Mesopor. Mater.*, **113**, 523 (2008).
13. M. Park, S.S. Park, M. Selvaraj, D.Y. Zhao and C.S. Ha, *Micropor. Mesopor. Mater.*, **124**, 76 (2009).
14. S.I. Matsuura, R. Ishii, T. Itoh, T. Hanaoka, S. Hamakawa, T. Tsunoda and F. Mizukami, *Micropor. Mesopor. Mater.*, **127**, 61 (2010).
15. J.X. Li, Z.Y. Xiong, L.H. Zhou, X. Han and H.L. Liu, *Micropor. Mesopor. Mater.*, **130**, 333 (2010).
16. Z.T. Zhang, S. Dai, X.D. Fan, D.A. Blom, S.J. Pennycook and Y. Wei, *J. Phys. Chem.*, **105B**, 6755 (2001).
17. Q.Z. Zhai and Y.C. Kim, *Chin. J. Spectros. Lab.*, **15**, 82 (1998).
18. W. Hammond, E. Prouzet, S.D. Mahanti, T.J. Pinnavaia, *Micropor. Mesopor. Mater.*, **27**, 19 (1999).
19. R. Kohn and M. Froba, *Catal. Today*, **68**, 227 (2001).
20. A.N. Shipway and I. Willner, *Chem. Phys. Chem.*, **1**, 18 (2000).
21. H. Weller, H.M. Schmidt, U. Koch, A. Fojtik, S. Baral, A. Henglein, W. Kunath, K. Weiss and D. Dieman, *Chem. Phys. Lett.*, **124**, 557 (1986).
22. Y. Wang and N. Herron, *Phys. Rev.*, **42B**, 7253 (1990).